Fig.S1

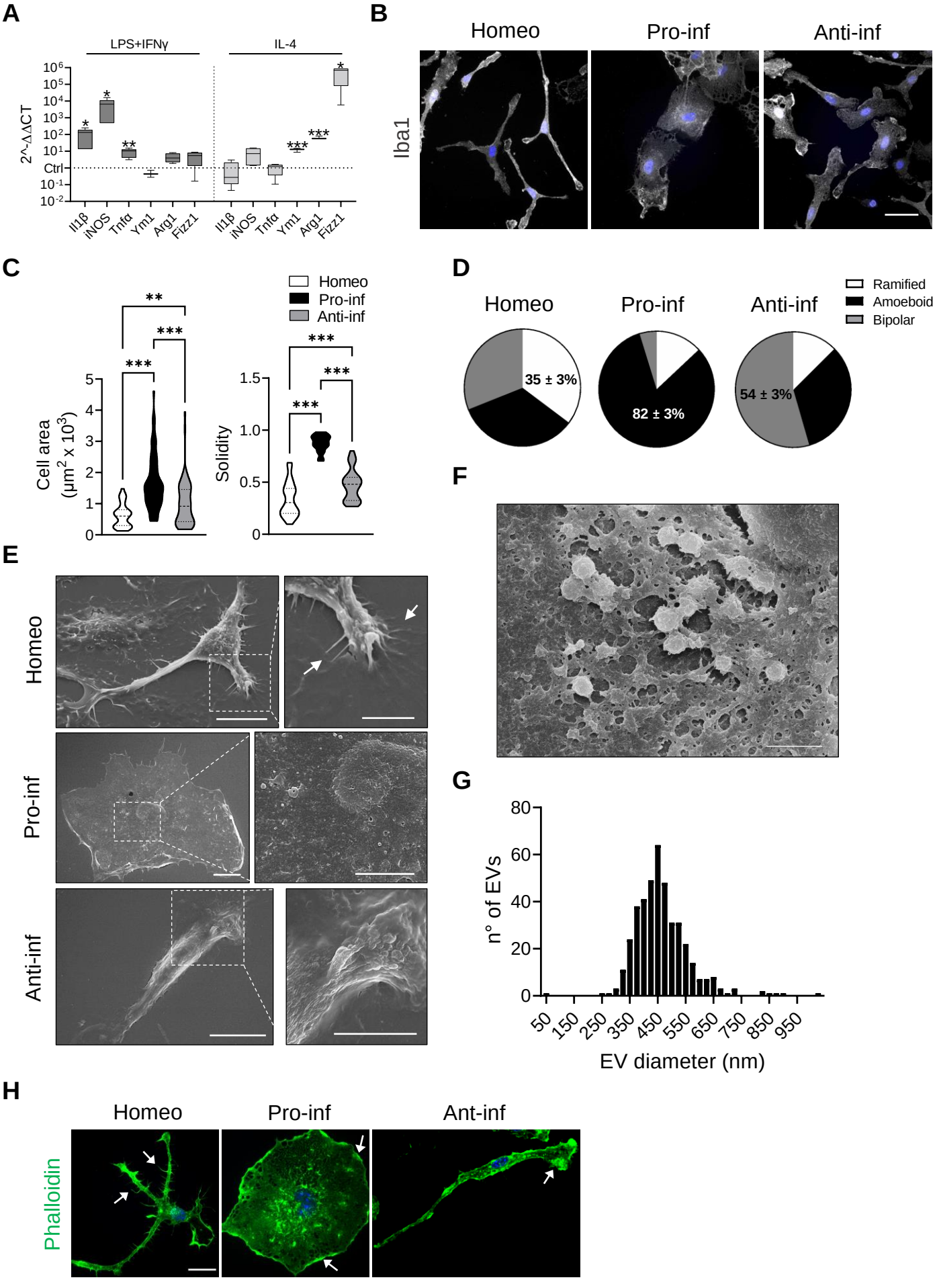
A
LPS+IFNγ
IL-4
2^-ΔΔCT
Ctrl
Il1β
iNOS
Tnfα
Ym1
Arg1
Fizz1
B
Homeo
Pro-inf
Anti-inf
Iba1
C
Homeo
Pro-inf
Anti-inf
Cell area (μm² x 10³)
Solidity
D
Homeo
Pro-inf
Anti-inf
Ramified
Amoeboid
Bipolar
35 ± 3%
82 ± 3%
54 ± 3%
E
Homeo
Pro-inf
Anti-inf
F
G
n° of EVs
EV diameter (nm)
H
Homeo
Pro-inf
Ant-inf
Phalloidin

Fig. S1. Molecular and morphological characterization of homeostatic, pro-inflammatory and anti-inflammatory primary microglia

(A) RT-qPCR reveals increased expression of pro-inflammatory (*Il1b, iNOS, Tnfα*) and anti-inflammatory genes (*Ym1, Arg1, Fizz1*) upon LPS-IFNγ or IL-4 challenge, respectively. Gene expression is normalized to the housekeeping gene *Gapdh,* n = 4 independent cultures. Box plots indicate the median, 25th, and 75th percentiles; whiskers show the minimum and maximum. *** p <0.001; ** p <0.01; *p <0.05, Student's t-test. **(B)** Representative images showing Iba1 immunostaining (gray) of microglia in CTRL (Homeo) condition and following LPS-IFNγ (Pro-inf) or IL4 (Anti-inf) treatment (Scale bar: 20 μm. Hoechst for nuclei visualization, blue). **(C)** Violin plots showing cell surface area (*left*) and solidity coefficient (*right*) related to Homeo (white), Pro-inf (black) and Anti-inf (gray) cells (n = 70 cells for each condition, from 3 independent experiments. *** p <0.001; **p <0.01. Kruskall-Wallis - Dunn's multiple comparisons test for cell area, *left*; One-way ANOVA - Tukey's multiple comparison test for solidity, *right*). **(D)** Pie charts illustrating the distribution of cell morphology in Homeo, Pro-inf and Anti-inf conditions. Ramified cells are enriched in Homeo (35 ± 3%), amoeboid in Pro-inf (82 ± 3%) and bipolar in Anti-inf (54 ± 3%), n = 3 independent experiments. **(E)** Representative scanning electron micrographs of microglia cells in Homeo (*top*), Pro-inf (*middle*) and Anti-inf (*bottom*) conditions. Ramified cells (Homeo) show filopodia extensions as indicated by arrows, ameboid cells (Pro-inf) exhibit numerous extracellular vesicles on the cell surface, while bipolar cells (Anti-inf) are characterized by extensive membrane ruffling on the cell surface and leading edge. Scale bar: 10 μm; zoom, 5 μm. **(F)** Scanning electron micrographs showing extracellular vesicles on the Pro-inf cell surface at higher magnification. Scale bar: 2 μm. **(G)** Distribution of EVs size measured on ameboid cell surface. n = 22 cells. **(H)** Representative confocal images of microglia labelled with Alexa Fluor 488-conjugated phalloidin (green). Ramified cells (Homeo) exhibit filopodia like structures (as indicated by arrows) while ameboid (Pro-inf) and bipolar cells (Anti-inf) are characterized by membrane ruffles along cell borders and at lamellipodia (as indicated by arrows). Scale bar: 25 μm. Hoechst for nuclei visualization, blue.

A

	Tyr+/EB+ comets	Tyr+/EB- comets	TOT
Homeo	96	57	153
Pro-inf	361	48	409
Anti-inf	146	33	179
TOT	603	138	741

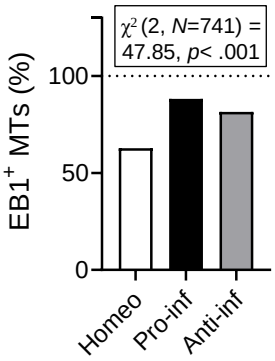

B

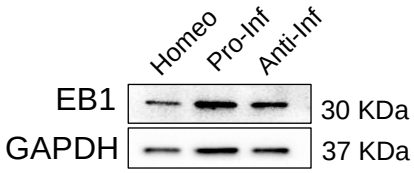

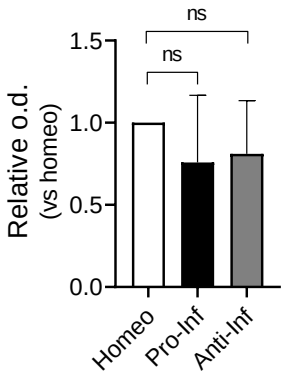

C

	Retrograde comets	Anterograde comets	TOT
Homeo	33	108	141
Pro-inf	1	187	188
Anti-inf	32	224	256
TOT	66	519	585

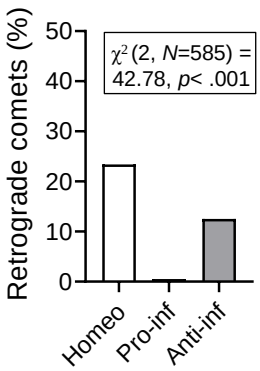

D

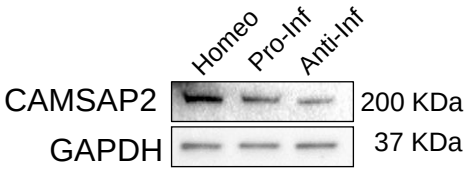

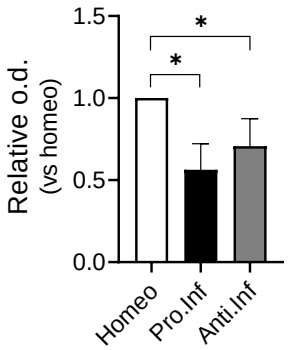

Fig. S2. Analysis of EB1 and CAMSAP2 expression in homeostatic, pro-inflammatory and anti-inflammatory microglia

(A) Contingency analysis of EB1 and tyrosinated a-tubulin (Tyr tub) co-staining in homeostatic (Homeo), pro-inflammatory (Pro-inf) and anti-inflammatory (Anti-inf) microglia: percentage of double positive staining are reported in the bar chart, χ^2 parameters are reported in the insert. (**B**) *Bottom*: bar chart reporting the amount of EB1 protein level in microglia phenotypes; *top*: representative immunoblot of EB1. Values are expressed as median ± interquartile range from 4 independent experiments. p=0.31, Mann Whitney test. (**C**) Contingency analysis of comets in Homeo, Pro-inf and Anti-inf microglia: percentage of retrograde comets are reported in the bar chart, χ^2 parameters are reported in the insert. (**D**) *Bottom*: bar chart reporting the amount of CAMSAP2 protein level in microglia phenotypes; *top*: representative immunoblot of CAMSAP2. Values are expressed as median ± interquartile range from 4 independent experiments. * $p < 0.05$, Mann Whitney test.

Fig.S3

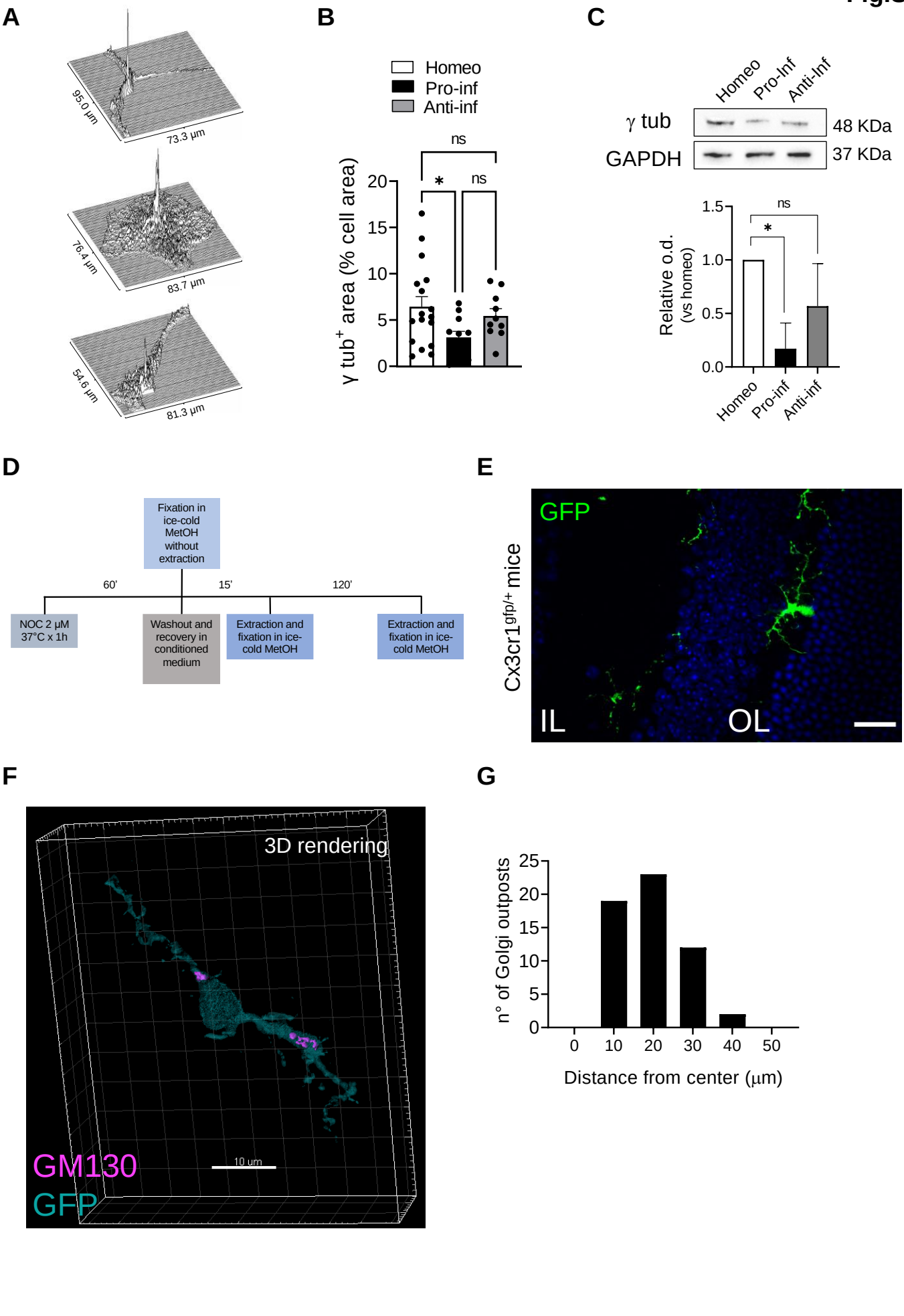
A
95.0 µm
73.3 µm
76.4 µm
83.7 µm
54.6 µm
81.3 µm
B
Homeo
Pro-inf
Anti-inf
ns
*
ns
γ tub+ area (% cell area)
20
15
10
5
0
C
Homeo
Pro-Inf
Anti-Inf
γ tub
GAPDH
48 KDa
37 KDa
ns
*
Relative o.d.
(vs homeo)
1.5
1.0
0.5
0.0
Homeo
Pro-inf
Anti-inf
D
Fixation in ice-cold MetOH without extraction
60'
15'
120'
NOC 2 µM 37°C x 1h
Washout and recovery in conditioned medium
Extraction and fixation in ice-cold MetOH
Extraction and fixation in ice-cold MetOH
E
GFP
Cx3cr1gfp/+ mice
IL
OL
F
3D rendering
GM130
GFP
10 µm
G
n° of Golgi outposts
25
20
15
10
5
0
0
10
20
30
40
50
Distance from center (µm)

Fig. S3. **Molecular, morphological and functional characterization of microglia non-centrosomal MTs nucleation in primary cultures and in retinal slices**

(A) Representative volumetric rendering of g-tubulin (γ tub) signal intensity of homeostatic (Homeo), pro-inflammatory (Pro-inf) and anti-inflammatory (Anti-inf) microglia. **(B)** Scatter dot plot showing analysis of γ tub signal over the cell area in Homeo, Pro-inf and Anti-inf microglia. Values are expressed as mean ± SEM (Homeo n = 17, Pro-inf n = 11 and Anti-inf n = 10 cells from 4 independent experiments). * $p < 0.05$, Kruskal-Wallis test - Dunn's multiple comparison test. **(C)** Representative immunoblot of total γ tub in Homeo, Pro-inf and Anti-inf microglia (*top*); bar chart showing the quantification of γ tub protein levels (*bottom*). Values are expressed as median ± interquartile range from 4 independent experiments. * $p < 0.05$, Mann Whitney test. **(D)** Treatment timeline of Nocodazole wash out assay. **(E)** Representative images of retinal slices (50 µm thickness) from control cx3cr1$^{gfp/+}$ mice stained with Hoechst for nuclei visualization (blue), showing retinal cell layers (IL inner layer, OL outer layer). Scale bar: 20 µm. **(F)** 3D rendering of sample retinal GFP+ microglia (cyan) stained for GM130 (magenta). Scale bar: 10 µm. **(G)** Bar chart reporting the number of Golgi outposts at increasing distance from the center of cell body in retinal microglia.

A

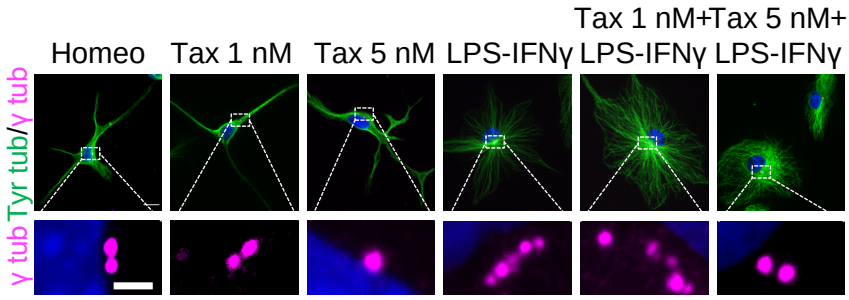

B

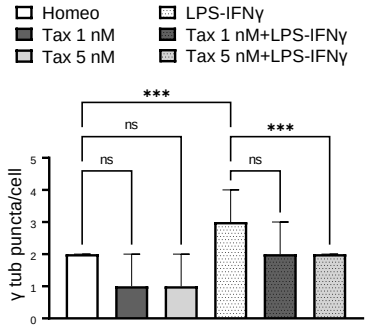

C

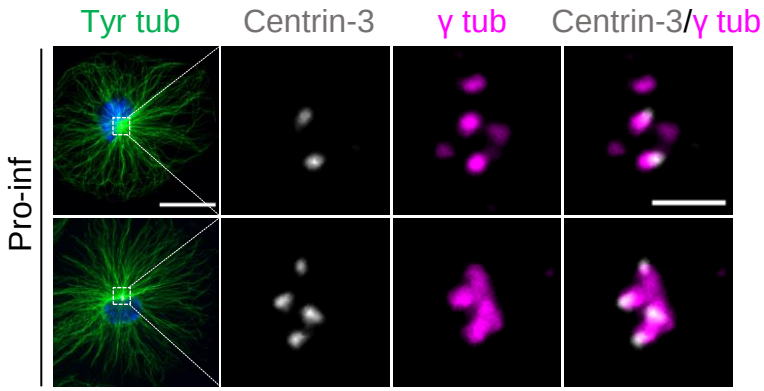

D

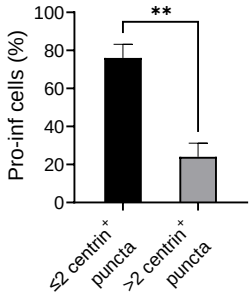

E

Cell cycle	Homeo	Pro-Inf
G1	83 ± 2	75 ± 4
S	8 ± 1	15 ± 2
G2/M	4 ± 1	8 ± 2

F

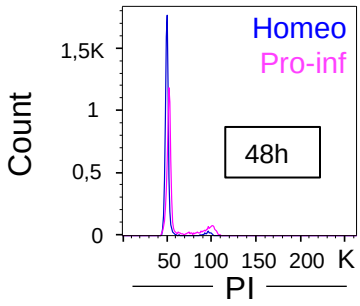

G

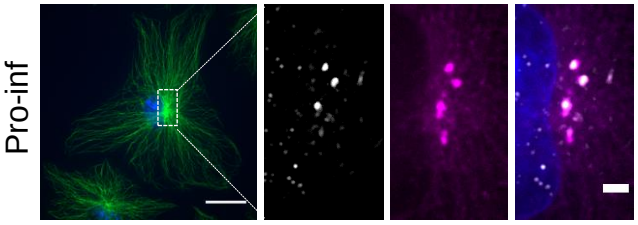

H

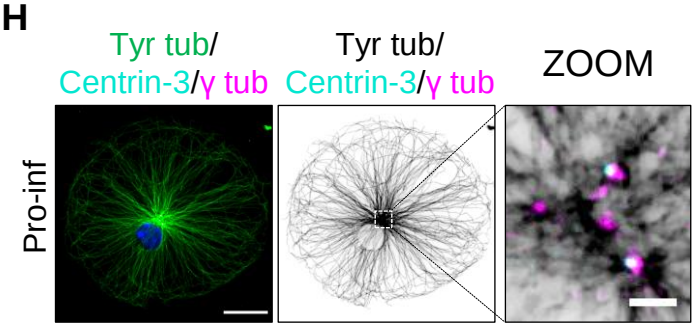

I

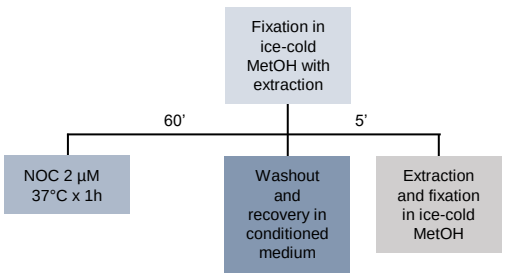

J

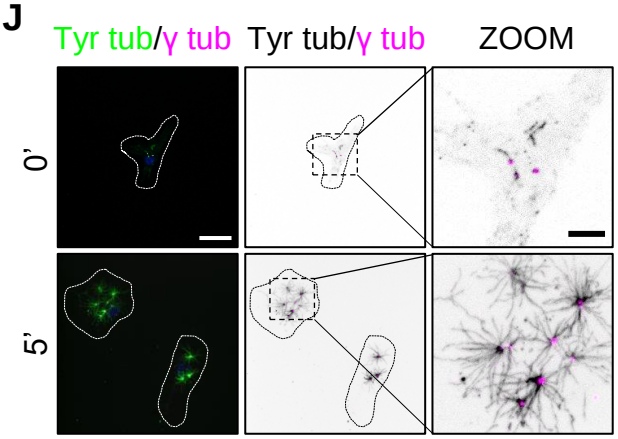

Fig. S4. Analysis of pericentriolar material maturation during microglia pro-inflammatory activation

(A) Representative images of immunostaining of tyrosinated (Tyr) tub (green) and g-tubulin (γ tub) (magenta) in homeostatic (Homeo), Taxol 1 nM treated (Tax 1 nM), Taxol 5 nM treated (Tax 5 nM), pro-inflammatory (LPS-IFNγ), Taxol 1 nM+LPS-IFNγ treated (Tax 1 nM+LPS-IFNγ) and Taxol 5 nM+LPS-IFNγ treated (Tax 5 nM+LPS-IFNγ) microglia (Top, Scale bar: 10 µm; zoom, 2 µm. Hoechst for nuclei visualization, blue). **(B)** Bar chart reporting the number of γ tub puncta per cell in homeostatic (Homeo), Taxol 1 nM treated (Tax 1 nM), Taxol 5 nM treated (Tax 5nM), pro-inflammatory (LPS-IFNγ), Taxol 1 nM+LPS-IFNγ treated (Tax 1 nM+LPS-IFNγ) and Taxol 5 nM+LPS-IFNγ treated (Tax 5nM+LPS-IFNγ) microglia. Values are expressed as median ± interquartile range from 3 independent experiments. ***p <0.001. Kruskall-Wallis - Dunn's multiple comparisons test. **(C)** Representative images showing Tyr tub (green), centrin-3 (gray) and γ tub (magenta) immunolabeling and co-localization of centrin-3 (gray) and γ tub (magenta) in pro-inflammatory (Pro-inf) microglia. Scale bar: 20 µm; zoom, 2 µm. Hoechst for nuclei visualization, blue. **(D)** Bar graph reporting the percentage of Pro-inf cells displaying ≤2 or >2 centrin^{+} puncta. Values are expressed as mean ± SEM of n = 52 cells from 3 independent experiments. **p <0.01, Student's t-test. **(E)** Table reporting the percentage of cells in G1, S and G2/M phases from Homeo and Pro-inf microglia cultures, stained with propidium iodide (PI) and analyzed by flow cytometry. Percentages indicate the relative enrichment in cell population, values are expressed as mean ± SEM from three independent experiments. **(F)** Representative histogram of cell cycle overlay of Homeo (blue line) and Pro-inf (magenta line) microglia. **(G)** Representative images showing Tyr tub (green), pericentrin (gray) and γ tub (magenta) immunolabeling in Pro-inf microglia. Scale bar: 20 µm; zoom, 2 µm. Hoechst for nuclei visualization, blue. **(H)** *Left:* representative image of Tyr tub (green), centrin-3 (cyan) and γ tub (magenta) immunolabeling in Pro-inf microglia. *Middle* and *right:* representative image showing Tyr tub (black, inverted LUT), centrin-3 (cyan) and γ tub (magenta) immunolabeling in Pro-inf microglia. Out of focus blur was removed using "remove haze" filter in Metamorph Software to highlight the asters. Scale bar: 20 µm; zoom, 2 µm. Hoechst for nuclei visualization, blue. **(I)** Treatment timeline of Nocodazole wash out assay. **(J)** Representative confocal images of the time course of the MT re-nucleation assay after nocodazole washout in Pro-inf microglia stained for Tyr tub (green) and γ tub (magenta). Scale bar: 20 µm; zoom: 5 µm. Hoechst for nuclei visualization, blue. Time 0' represents the MT depolymerizing effect of nocodazole in Pro-inf cells with free tubulin extraction.

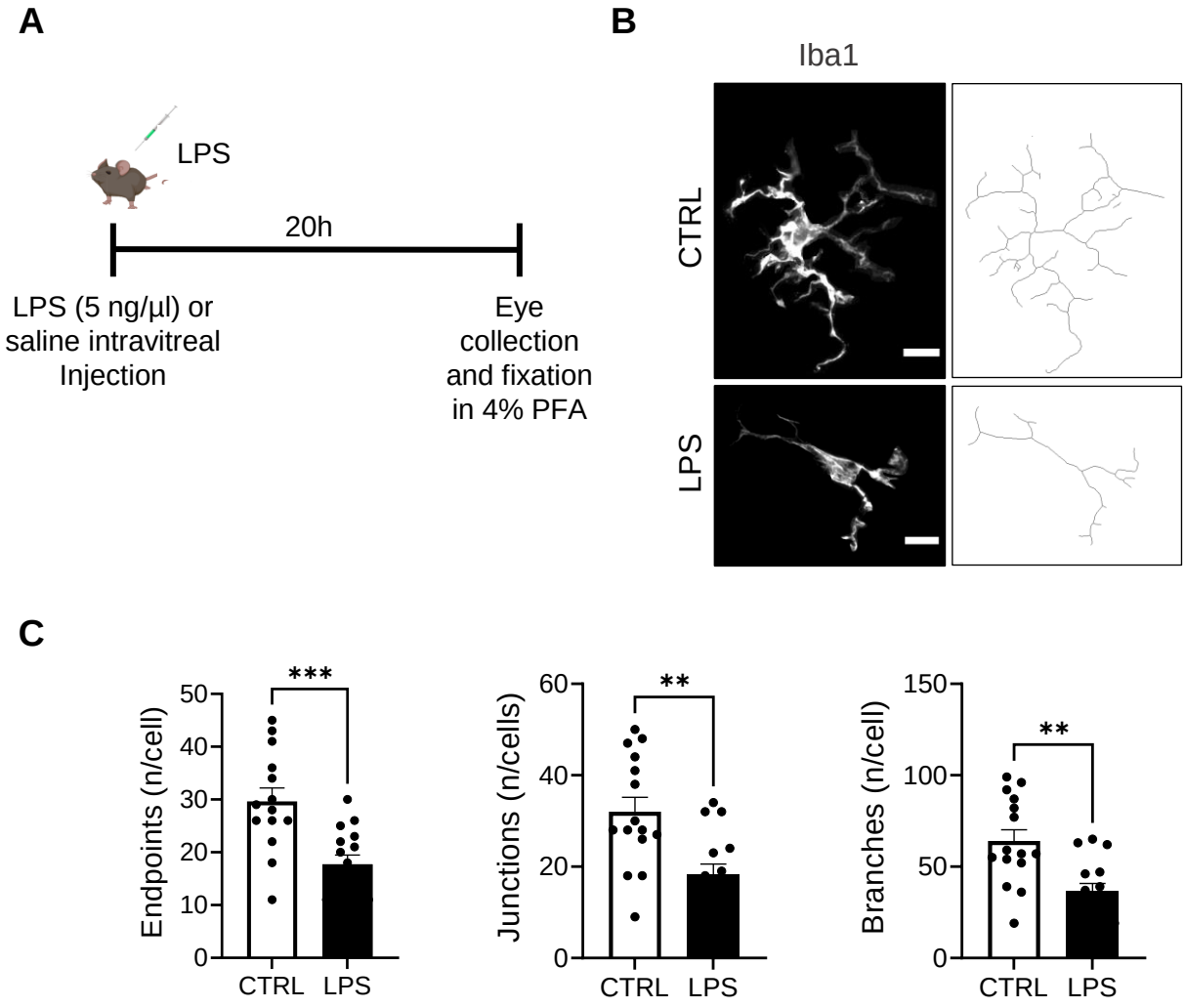
A
LPS
20h
LPS (5 ng/µl) or saline intravitreal Injection
Eye collection and fixation in 4% PFA
B
Iba1
CTRL
LPS
C
Endpoints (n/cell)
***
CTRL
LPS
Junctions (n/cells)
**
Branches (n/cell)
**

Fig. S5. Characterization of *in vivo* microglia activation in the LPS-induced uveitis model

(A) Schematic illustration of surgical procedure and tissue collection. **(B)** *Left*: representative immunofluorescence images of microglia (Iba1, gray) in retinal slices (50 µm thickness) from CTRL (sham) and LPS treated mice. Scale bar: 10 µm. *Right*: corresponding skeletonized images. **(C)** Scatter dot plots reporting microglia arborization parameters as endpoints (*left*), junctions (*middle*) and branches (*right*) obtained from skeleton analysis of retinal microglia from CTRL (sham) and LPS treated mice. Values are expressed as mean ± SEM (CTRL, n = 14/3 cells/mice; LPS, n = 15/3 cells/mice; *** p <0.001, ** p <0.01; Student's t-test.

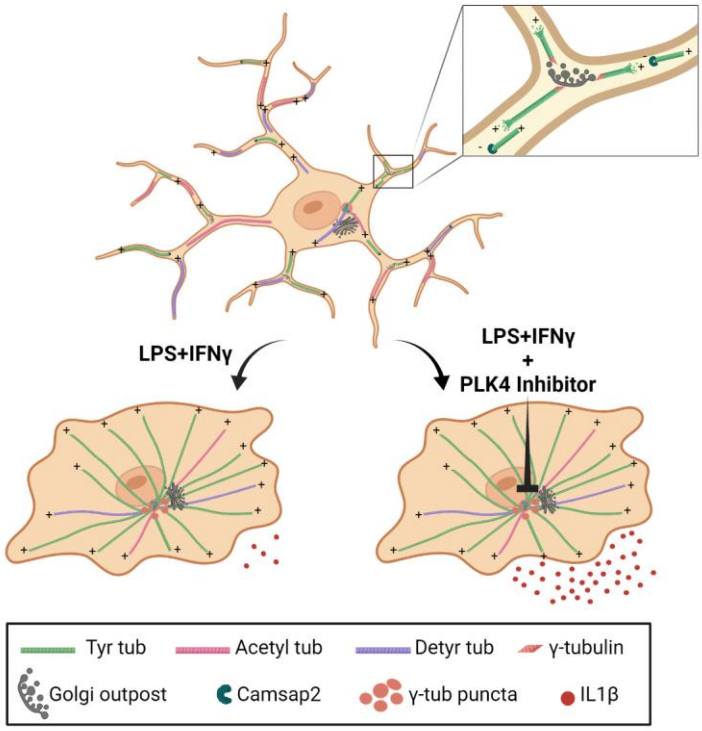
LPS+IFNγ
LPS+IFNγ
+
PLK4 Inhibitor
Tyr tub
Acetyl tub
Detyr tub
γ-tubulin
Golgi outpost
Camsap2
γ-tub puncta
IL1β

Fig. S6. Graphical abstract to illustrate the main findings of this study. Homeostatic microglia have stable MT arrays, while microglia reactivity increases MT dynamic behavior. In addition, homeostatic microglia have non-centrosomal MTs with mixed polarity similar to the architecture of highly specialized cells such as neurons and oligodendrocytes. Pro-inflammatory microglia reactivity results in restricted g-tubulin localization to puncta around the centrosome because of *de novo* pericentriolar material (PCM) maturation. Inhibition of PCM maturation by Polo-like Kinase 4 (PLK4) in pro-inflammatory microglia stimulates IL-1b release.

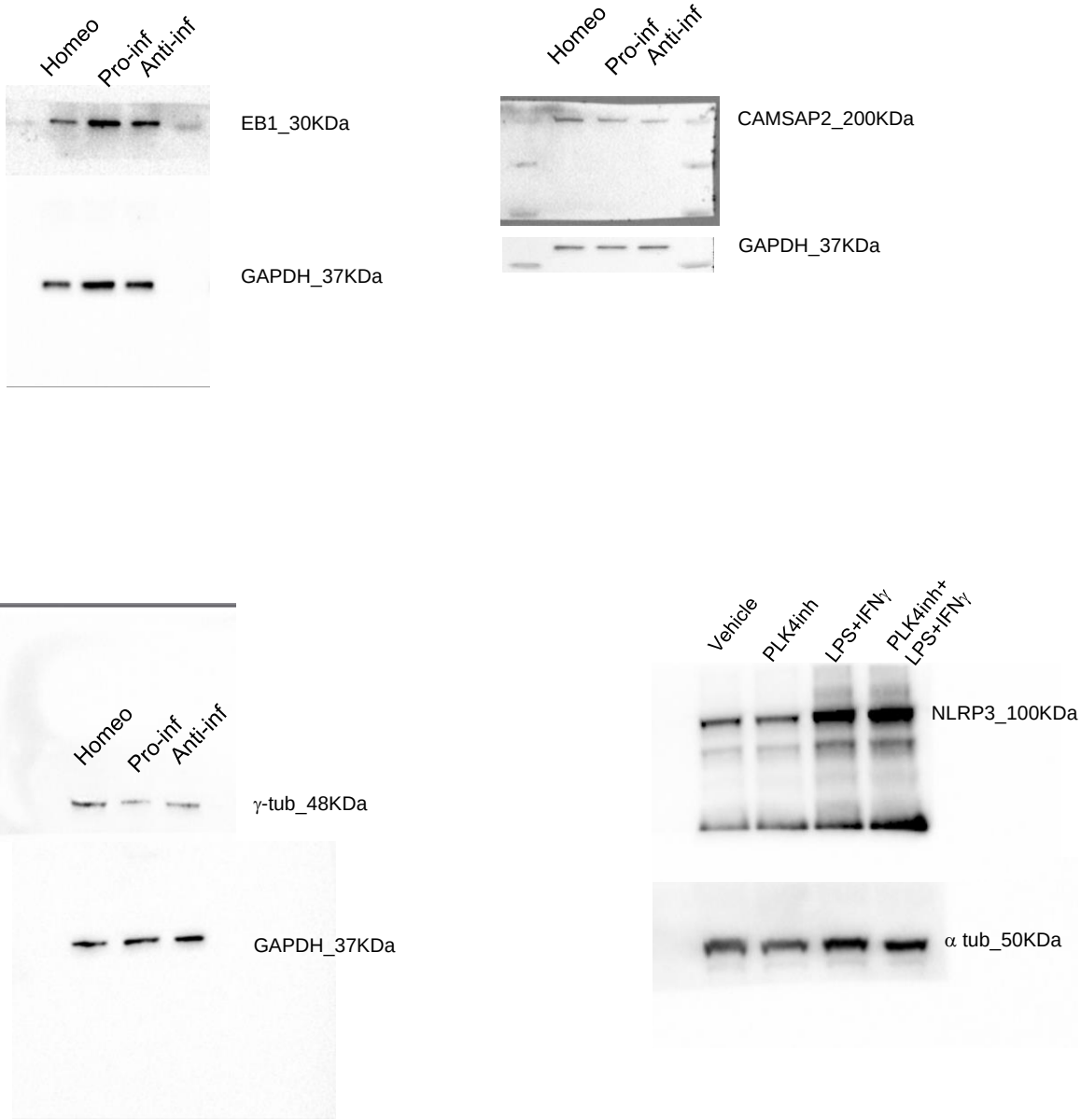

Fig S7: Original western blots